

GUARANTEED METHOD FOR THE ESTIMATION OF DIELECTRIC RELAXATION MODEL PARAMETERS

T. RAÏSSI, N. RAMDANI, L. IBOS and Y. CANDAU

CERTES, EA3481, University Paris XII Val de Marne, 61 avenue du Général de Gaulle, Créteil, 94010, France
e-mail : {raissi ; ramdani ; ibos ; candau}@univ-paris12.fr

Abstract – In this paper, a guaranteed method for the estimation of dielectric relaxation model parameters is presented. The only assumption used is that data uncertainty is bounded with known prior bounds. The main difference with classical methods based on least squares minimisation is that the solution is not a point but leads to a set. When least squares methods are used, the model structure should be known. In some cases, this information is not available (for instance because there is not enough data); in this case the identification process can lead to unacceptable results. In this paper, a new technique, based on interval analysis, allowing the rejection of models that are not consistent with data is presented. When a solution exists, the guaranteed method provides a natural description of the uncertainty associated with the identified dielectric parameters.

1. INTRODUCTION

Measurement methods such as broadband dielectric spectroscopy, are nowadays useful for the study of organic or inorganic insulating materials, owing to the large frequency domain that can be explored. In the case of polymeric materials, in the frequency range $[10^{-3} \text{ Hz}; 10^7 \text{ Hz}]$, dielectric relaxation spectra can be split into a sum of independent contributions, the so-called relaxation modes, corresponding to dipole motions of the macromolecular chains [1]. Dielectric relaxation spectra can be approximated using semi-empirical models derived from the Debye equation, such as Cole-Cole, Cole-Davidson or Havriliak-Negami laws [2]. In this work, we consider only the Havriliak-Negami model, given by the following expression [3]:

$$\varepsilon(\omega) = \varepsilon_{\infty} + \sum_{i=1}^n \frac{\Delta\varepsilon_i}{\left(1 + (j\omega\tau_i)^{\alpha_i}\right)^{\beta_i}} + \frac{\sigma_0}{\varepsilon_0 (j\omega)^s} \quad (1)$$

where $\varepsilon(\omega)$ is the relative dielectric complex permittivity measured at a constant temperature and pulsation ω , ε_{∞} is the high frequency permittivity, τ_i and $\Delta\varepsilon_i$ are respectively the relaxation time and the dielectric strength associated with relaxation mode i , α_i and β_i are shape parameters describing respectively the symmetric and the asymmetric broadening of the distribution function of relaxation times and n is the number of relaxation modes in the dielectric spectrum. In equation (1), the last term allows to take into account the DC ohmic contribution in the low frequencies domain, where σ_0 is the DC conductivity, s is an adjustable parameter (with $0 < s \leq 1$) and ε_0 is the vacuum dielectric permittivity.

Dielectric permittivity can be decomposed into a real part ε' and an imaginary part ε'' as follows

$$\varepsilon(\omega) = \varepsilon'(\omega) - j\varepsilon''(\omega) \quad (2)$$

where the real part is given by

$$\varepsilon'(\omega) = \varepsilon_{\infty} + \sum_{i=1}^n \left[\Delta\varepsilon_i \frac{\cos(\beta_i\varphi_i)}{\left(1 + 2(\omega\tau_i)^{\alpha_i} \sin\left(\frac{\pi(1-\alpha_i)}{2}\right) + (\omega\tau_i)^{2\alpha_i}\right)^{\beta_i/2}} \right] + \frac{\sigma_0}{\varepsilon_0} \omega^{-s} \cos\left(\frac{\pi s}{2}\right) \quad (3)$$

and the imaginary part by

$$\varepsilon''(\omega) = \sum_{i=1}^n \left[\Delta\varepsilon_i \frac{\sin(\beta_i\varphi_i)}{\left(1 + 2(\omega\tau_i)^{\alpha_i} \sin\left(\frac{\pi(1-\alpha_i)}{2}\right) + (\omega\tau_i)^{2\alpha_i}\right)^{\beta_i/2}} \right] + \frac{\sigma_0}{\varepsilon_0} \omega^{-s} \sin\left(\frac{\pi s}{2}\right) \quad (4)$$

with

$$\varphi_i = \arctan \left[(\omega\tau_i)^{\alpha_i} \cos\left(\frac{\pi(1-\alpha_i)}{2}\right) \right] / \left[1 + (\omega\tau_i)^{\alpha_i} \sin\left(\frac{\pi(1-\alpha_i)}{2}\right) \right] \quad (5)$$

The number of relaxation processes n is usually not greater than 3. The dielectric parameters usually satisfy the following constraints

$$\varepsilon_\infty > 1, \Delta\varepsilon_i > 0, \tau_i > 0, \alpha_i \in]0,1], \beta_i \in]0,1], \sigma_0 \geq 0, s \in]0,1], \text{ for } i = 1 \text{ to } n \quad (6)$$

However, parameters σ_0 and s will not be taken into account in the following which is equivalent to assume $\sigma_0 = 0$.

In many cases (narrow frequency domain, relaxation modes overlapping, noisy data or predominant DC ohmic contribution), the precise estimation of these parameters using classical least-squares minimisation methods becomes a hard exercise. The aim of this paper is to give a guaranteed method for estimating the parameters $\mathbf{p} = (\varepsilon_\infty, \tau_i, \alpha_i, \beta_i, \Delta\varepsilon_i)^T$ in the sense that no solution can be lost. This property is an important advantage compared to local iterative techniques such as the quasi-Newton or the conjugate gradient methods, as the solution they return depends on the initial value given to the parameters. In this paper, we show how to derive guaranteed results, where the solutions are given by some sets guaranteed to contain the actual solutions. These sets are then used to characterise the identified parameters uncertainty. The main tools to be used to solve the parameter estimation problem are interval analysis [4] and set inversion [5].

2. BOUNDED ERROR CONTEXT

We denote by ε_m the theoretical relative dielectric complex permittivity obtained by using the model (1), and by $\hat{\varepsilon}$ the experimental measured permittivity. Let e be the measurement error ($e = \hat{\varepsilon} - \varepsilon_m$), then a set $[\varepsilon]$ containing the acceptable ε is built as:

$$[\varepsilon] = [\hat{\varepsilon} - e, \hat{\varepsilon} + e] \quad (7)$$

Estimating the parameter vector \mathbf{p} in a bounded error context consists in determining the set \mathbb{S} of all the parameters \mathbf{p} contained in the prior search set \mathbb{P} such that theoretical $\varepsilon_m(\omega)$ (for all the ω) are consistent with the experimental data and with the uncertainty. It means that the error between the theoretical and the experimental data remains acceptable for all ω_j . The solution set \mathbb{S} is thus given by:

$$\mathbb{S} = \{ \mathbf{p} \in \mathbb{P} \mid \varepsilon_m(\mathbf{p}) \in [\varepsilon] \} \quad (8)$$

The characterization of the solution set \mathbb{S} is a set inversion problem; a guaranteed approximation of such a set can be provided by using interval analysis.

2.1 Interval Analysis

An interval, denoted by $[x]$, is a connected and closed subset of \mathbb{R} . The set of all real intervals is denoted by \mathbb{IR} . Real operations such as addition, subtraction, multiplication and division are extended to intervals according to the following formula:

$$[x] \circ [y] = \{ x \circ y \mid x \in [x] \text{ et } y \in [y] \} \quad (9)$$

where $\circ \in \{+, -, \times, /\}$. Given an interval $[x] = [x, \bar{x}]$, the following entities are defined: width: $w([x]) = \bar{x} - x$; midpoint: $m([x]) = (\bar{x} + x) / 2$.

We denote by a box \mathbf{x} a vector with interval elements; its width and midpoint are defined componentwise. As arithmetic operations, real functions are extended to intervals. Let f be a function from \mathbb{R} to \mathbb{R} , the interval function $[f]$ from \mathbb{IR} to \mathbb{IR} is called an inclusion function of f if and only if:

$$\forall [x] \in \mathbb{IR}, f([x]) \subseteq [f]([x]) \quad (10)$$

The inclusion function is not unique, and the optimal one is the interval function giving the smallest evaluation. In most cases, the optimal inclusion function is not available and the natural inclusion one is used instead; the latter is obtained by replacing all real arguments by their interval counterparts and elementary real functions (such as \sin , \cos , \log , ...) by their extensions to intervals (see [4] for more details).

SIVIA

SIVIA (Set Inversion Via Interval Analysis, [5]), based on interval analysis, allows the characterization of the solution set \mathbb{S} by computing two sets $\underline{\mathbb{S}}$ and $\overline{\mathbb{S}}$ such as:

$$\underline{\mathbb{S}} \subseteq \mathbb{S} \subseteq \overline{\mathbb{S}} \quad (11)$$

The set $\underline{\mathbb{S}}$ contains all the boxes proved to be feasible and $\overline{\mathbb{S}}$ contains $\underline{\mathbb{S}}$ and the undetermined boxes.

Let ε_m be the actual model output and N the number of measurements, then, a box $[\mathbf{p}]$ is called:

- feasible, if $[\varepsilon_m(\mathbf{p}, \omega_j)] \subseteq [\varepsilon(\omega_j)]$, $j=1, \dots, N$
- unfeasible, if $\exists j \mid [\varepsilon_m(\mathbf{p}, \omega_j)] \cap [\varepsilon(\omega_j)] = \emptyset$
- undetermined, otherwise.

Algorithm SIVIA(in : $[\mathbf{p}], [\varepsilon], \eta$; inout : $\underline{\mathbb{S}}, \bar{\mathbb{S}}$)

- 1 if $[\varepsilon_m(\mathbf{p})] \cap [\varepsilon] = \emptyset$, reject $[\mathbf{p}]$;
- 2 if $[\varepsilon_m(\mathbf{p})] \subseteq [\varepsilon]$, $\underline{\mathbb{S}} := \underline{\mathbb{S}} \cup [\mathbf{p}]$; $\bar{\mathbb{S}} := \bar{\mathbb{S}} \cup [\mathbf{p}]$;
- 3 if $w([\mathbf{p}]) < \eta$ $\bar{\mathbb{S}} := \bar{\mathbb{S}} \cup [\mathbf{p}]$;
- 4 bisect $[\mathbf{p}]$ on $[\mathbf{p}_1]$ and $[\mathbf{p}_2]$;
- 5 SIVIA(in : $[\mathbf{p}_1], [\varepsilon], \eta$; inout : $\underline{\mathbb{S}}, \bar{\mathbb{S}}$); SIVIA(in : $[\mathbf{p}_2], [\varepsilon], \eta$; inout : $\underline{\mathbb{S}}, \bar{\mathbb{S}}$);

The parameter η in SIVIA is used to stop the bisection if a box is too small. SIVIA is a branch-and-bound algorithm, its complexity is exponential with the number of parameters to be estimated, which means that it is efficient only when the dimension of \mathbf{p} is low. To reduce the number of bisections in SIVIA, constraint propagation techniques [6,7,8] are used. These techniques make it possible to reduce the search box without making bisections.

2.2 Constraints satisfaction problem

Definition 1 – CSP: Consider n variables $x_i \in \mathbb{R}$, $i \in \{1, 2, \dots, n\}$, linked by n_f relations of the form :

$$f_j(x_1, x_2, \dots, x_n) = 0, \text{ for } j = 1 \text{ to } n_f \quad (12)$$

and where each variable x_i is known to belong to a prior interval domain $[x_i]_0$; define the vector $\mathbf{x} = (x_1, x_2, \dots, x_n)^T$ and the function $\mathbf{f}(\mathbf{x}) = (f_1(\mathbf{x}), f_2(\mathbf{x}), \dots, f_{n_f}(\mathbf{x}))^T$, then eqn.(12) can be written as a *constraint satisfaction problem (CSP)* [7] :

$$H : \mathbf{f}(\mathbf{x}) = \mathbf{0}, \quad \mathbf{x} \in [\mathbf{x}]_0 \quad (13)$$

Definition 2 – Contractors: Interval CSPs can be solved with contractors. An operator C_H is a contractor for the CSP H defined by (13) if, for any box $[\mathbf{x}]$ in $[\mathbf{x}]_0$, it satisfies:

$$\begin{aligned} C_H([\mathbf{x}]) &\subset [\mathbf{x}] && \text{(contractance)} \\ C_H([\mathbf{x}]) \cap \mathbb{S} &= [\mathbf{x}] \cap \mathbb{S} && \text{(correctness)} \end{aligned} \quad (14)$$

where \cap is the intersection of two boxes and \mathbb{S} a solution set for H .

Definition 3 – Solver: A solver for the CSP defined by (13) is an algorithm Ψ such that:

$$\mathbf{f}(\mathbf{x}) = \mathbf{0} \Leftrightarrow \mathbf{x} = \Psi(\mathbf{x}) \quad (15)$$

According to the fixed-point theorem and using (15), if the series $\mathbf{x}_{k+1} = \Psi(\mathbf{x}_k)$ converges towards \mathbf{x}_∞ , then \mathbf{x}_∞ shall contain the solution of H .

Several punctual solvers such as the Newton method, the Gauss-Siedel or the Krawczyk operators have been extended to intervals, and are used to solve efficiently even non-linear CSPs [7, 9]. However, they remain limited to problems where the number of constraints is equal to the number of variables.

When the number of constraints and the number of variables are different, one can use an alternate contractor relying on interval propagation techniques. These techniques combine the constraint propagation techniques classically used in the domain of artificial intelligence [6] and interval analysis. They have been brought to automatic control in [8], for solving set inversion problems in a bounded-error context. The algorithm used for constraint propagation is based on the interval extension of the local Walz filtering [6, 8]. In fact, the relationships (12) between the variables can be viewed as a network where the nodes are connected with the constraints. In order to spread the consequences of each node throughout the network, the main idea is to deal with a local group of constraints and nodes and then record the changes in the network. Further deductions will make use of these changes to make further changes. The inconsistent values for the state vector are thus removed. If the network exhibits no cycles, then optimal filtering can be achieved by performing only one forward and one backward propagation: this is known as the *forward-backward contractor* [7].

2.3 Example: The forward-backward contractor

Consider the CSP

$$H : f(\mathbf{x}) = \mathbf{0}, \quad \mathbf{x} \in [\mathbf{x}]_0 \quad (16)$$

where $f(\mathbf{x}) = x_3 - x_2 \cdot x_1$ and the prior domain $[\mathbf{x}]_0 = [2, 10] \times [1, 10] \times [1, 5]$. The constraint f can be rewritten as:

$$x_3 = x_2 \cdot x_1 \quad (17)$$

The forward interval constraint propagation will remove all inconsistent values from x_3 , as follows

$$[x_3]_1 = ([x_1]_0 \cdot [x_2]_0) \cap [x_3]_0 = [2, 5] \quad (18)$$

Then, the backward interval constraint propagation will remove all inconsistent values from x_1 and x_2 as follows

$$[x_1]_1 = ([x_3]_1 / [x_2]_0) \cap [x_1]_0 = [2, 5] \quad (19)$$

$$[x_2]_1 = ([x_3]_1 / [x_1]_1) \cap [x_2]_0 = [1, \frac{5}{2}] \quad (20)$$

If the operations (18)-(20) are performed again, the intervals would not be modified. The box $[\mathbf{x}]_1 = [2, 5] \times [1, \frac{5}{2}] \times [2, 5]$ contains the solution of the CSP. For more details about this contractor see [7].

3. A CASE STUDY WITH A SINGLE RELAXATION

In this section, we study the case of single relaxation spectra. The pseudo-actual data are obtained by simulating the Havriliak-Negami model with a single relaxation process, *i.e.* equations (3) and (4) are used with $n = 1$.

3.1 Relaxation parameters

We used three relaxation spectra labelled ‘‘cases A, B and C’’, see Figure 1. For these three cases, α , β , $\Delta\epsilon$ and ϵ_∞ parameters are identical and are given in Table 1.

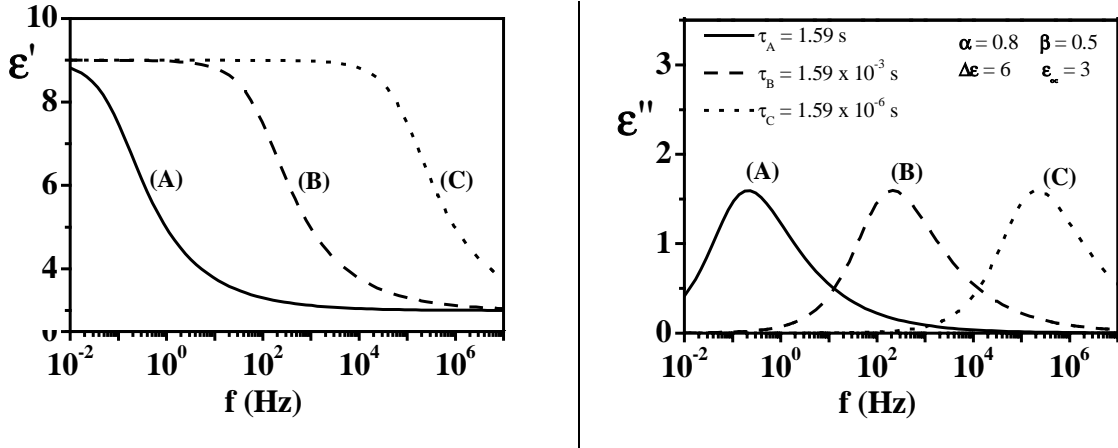


Figure 1. Real and imaginary parts of the relative dielectric permittivity for simulation cases A, B and C.

Table 1. α , β , $\Delta\epsilon$ and ϵ_∞ parameters values used for single relaxation spectra.

α	β	$\Delta\epsilon$	ϵ_∞
0.8	0.5	6	3

3.2 Influence of frequency windowing

In order to take into account the effect of frequency windowing on the estimation, we used three different values of the relaxation time τ . The values corresponding to ‘‘cases A, B and C’’ are reported in Table 2. The corresponding dielectric spectra are presented in Figure 1. The width of each interval quantifies the uncertainty on the corresponding identified parameter.

Table 2. Relaxation time values corresponding to cases A, B and C.

Case	A	B	C
τ (s)	1.59	1.59×10^{-3}	1.59×10^{-6}

Table 3. Estimated parameters and computing time values corresponding to cases A, B and C.

Case	A	B	C
α	[0.7767 ; 0.8195]	[0.7958 ; 0.8045]	[0.7981 ; 0.8021]
β	[0.4829 ; 0.5220]	[0.4919 ; 0.5078]	[0.4861 ; 0.5146]
$\Delta\varepsilon$	[5.918 ; 6.0862]	[5.9352 ; 6.0667]	[5.9413 ; 6.0656]
τ (s)	[1.4725 ; 1.7028]	[1.52 ; 1.67] 10^{-3}	[1.51 ; 1.67] 10^{-6}
ε_{∞}	[2.9844 ; 3.0156]	[2.9806 ; 3.0188]	[2.9393 ; 3.0358]
C.T. (s)	428	53	50

The parameters estimated for the simulation cases A, B and C are given in Table 3 along with the computing time (C.T.) obtained using a PC with a Celeron™ 733 MHz processor. For these simulations, the amplitude of the noise was fixed to 0.5% for both real and imaginary parts of the dielectric permittivity. The parameter values obtained are not single values but real intervals, the width of which quantifies the uncertainty in the identified parameter.

As expected, the smallest intervals, i.e. the smallest uncertainties, are obtained for case B, i.e. when the pseudo-experimental data include the whole relaxation process. On the contrary, the largest intervals are obtained when the low frequency part of the relaxation process is truncated, excepted for ε_{∞} which is the worst estimated parameter when the high frequency part of the relaxation process is truncated. Nevertheless, in all cases, the true parameters values are included in the solution intervals, with a rather acceptable computing time.

3.3 Influence of signal to noise ratio

In order to take into account the influence of signal to noise ratio on the identified parameters uncertainty, we performed several estimations using the simulation case B for three different noise amplitudes: 1%, 2% and 5%. The results obtained are reported in Table 4.

Table 4. Estimated parameters and computing time values corresponding to noise amplitude (N.A.) values of 1%, 2% and 5%.

N.A.	1%	2%	5%
α	[0.793;0.807]	[0.790;0.810]	[0.781;0.820]
β	[0.487;0.513]	[0.480;0.519]	[0.461;0.538]
$\Delta\varepsilon$	[5.890;6.115]	[5.816;6.189]	[5.628;6.389]
τ (ms)	[1.490;1.694]	[1.427;1.783]	[1.277;2.010]
ε_{∞}	[2.963;3.035]	[2.931;3.068]	[2.832;3.164]
C.T.	108 s	454 s	2h 22min

We can notice that increasing the noise amplitude induces as expected a pessimistic estimation of the model parameters. This is particularly true for β , τ and $\Delta\varepsilon$ parameters, whereas α and ε_{∞} are less affected by a strong increase of the noise amplitude.

Besides, a dramatic increase of the computing time is observed for a noise amplitude equal to 5%. This can be explained by the fact that larger prior error bounds on model output render the contractor less efficient and thus make necessary a greater number of bisections.

4. CASE STUDY WITH TWO RELAXATION PROCESSES

In this section, we study the case of two relaxation spectra. The pseudo-actual data are obtained by simulating a Havriliak-Negami model with two relaxation processes.

4.1 Relaxation parameters and simulation cases

In this part, we are interested in the estimation of Havriliak-Negami model parameters when two relaxation processes are observed in the pseudo-actual measurement frequency range. The higher and lower frequency relaxation modes will be named respectively “relaxation 1” (subscript 1) and “relaxation 2” (subscript 2). Four simulation cases have been considered. Eight of the nine parameters were kept constant for all simulations. These parameters are given in Table 5 (see also Figure 2).

Table 5. Constant parameters values used for two relaxation spectra simulations.

α_1	β_1	$\Delta\epsilon_1$	α_2	β_2	$\Delta\epsilon_2$	τ_2 (s)	ϵ_∞
0.6	1	1	0.8	0.7	6	0.15915	3

The noise amplitude was fixed to 0.5%. The only parameter that was changed is the relaxation time τ_1 associated with “relaxation 1”. In fact, we decided to change the ratio of the two relaxation times values τ_2/τ_1 in order to show the influence of the modes overlapping upon the parameters estimation. The corresponding values of τ_1 are given in Table 6. The dielectric spectra investigated are plotted in Figure 2.

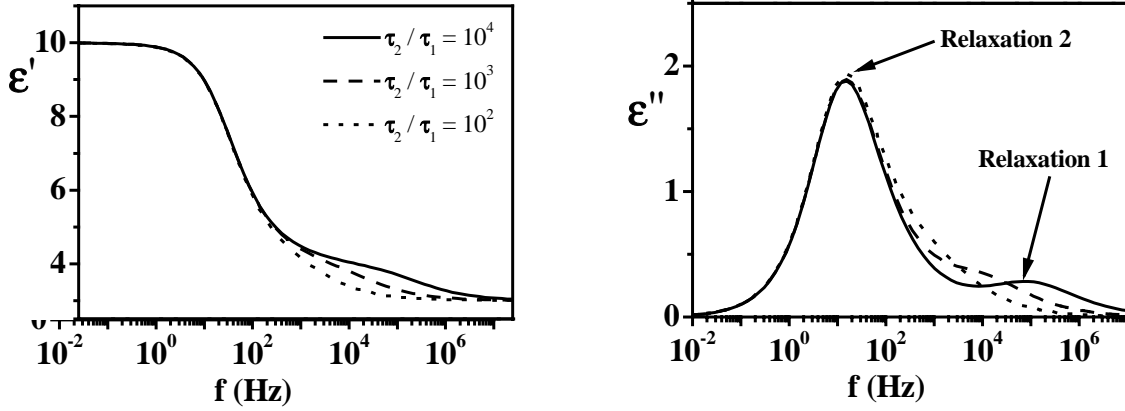


Figure 2. Real and imaginary parts of the relative dielectric permittivity for the two relaxation processes simulation cases.

Table 6. τ_2/τ_1 and τ_1 values used for two relaxation spectra simulations.

τ_2/τ_1	10^4	10^3	10^2	10
τ_1 ($\times 10^{-6}$ s)	15.915	159.15	1591.5	15915

4.2 Model invalidation – selection of the number of relaxation processes

When two relaxation processes overlap, it is difficult to determine the number of terms in eqn.(1), i.e. the number of relaxation processes to impose in the model.

If a classical optimisation method, such as least-square minimisation, is used to estimate the model parameters, it is almost impossible to invalidate the model proposed. In Figure 3, we present in a Cole-Cole plot the dielectric relaxation spectrum corresponding to the considered simulation case (two relaxation processes), using $\tau_2/\tau_1 = 10$, along with the identified model with least squares, using the Havriliak-Negami model with a single relaxation process. The optimal parameters obtained by least-square minimisation are: $\epsilon_\infty = 3.01$; $\Delta\epsilon = 6.9874$; $\tau = 0.402$ s; $\alpha = 0.76$; $\beta = 0.73$. This result is visually quite acceptable.

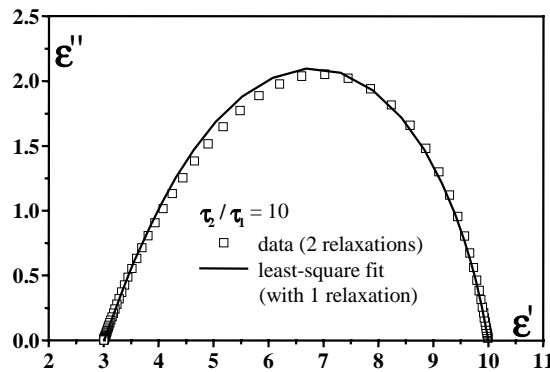


Figure 3. Cole-Cole plot of the two relaxation processes simulation case with $\tau_2/\tau_1 = 10$.

On the contrary, the bounded error approach introduced in this paper proves that no solution is found with a single relaxation model, the latter is thus invalid. In next section, the bounded error identified is performed with a two relaxations model.

4.3 A two relaxation model - Influence of modes overlapping on the parameters estimation

In the following, we used a two relaxation model. The estimated parameters and the corresponding computing times are reported in Table 7 for the four dielectric relaxation spectra studied. We must note that the width of the estimated parameter intervals increases when the ratio τ_2/τ_1 is decreased, i.e. when the two relaxation processes are overlapped. This is particularly true for the fastest relaxation, because of its lower dielectric strength. Finally, we can notice that the ε_∞ parameter is always rather well estimated in all cases.

Table 7. Estimated parameters and computing time values corresponding to τ_2/τ_1 values of 10^4 , 10^3 and 10^2 .

τ_2/τ_1	10^4	10^3	10^2
α_1	[0.593 ; 0.633]	[0.593 ; 0.654]	[0.578 ; 0.687]
β_1	[0.9375 ; 1]	[0.908 ; 1]	[0.846 ; 1]
$\Delta\varepsilon_1$	[0.971 ; 1.015]	[0.907 ; 1.061]	[0.792 ; 1.304]
$\tau_1 (\times 10^{-6} \text{ s})$	[15.04 ; 17.39]	[138.5 ; 187.5]	[1145 ; 2348]
α_2	[0.796 ; 0.803]	[0.796 ; 0.803]	[0.792 ; 0.810]
β_2	[0.683 ; 0.713]	[0.672 ; 0.727]	[0.674 ; 0.778]
$\Delta\varepsilon_2$	[5.984 ; 6.029]	[5.939 ; 6.095]	[5.696 ; 6.211]
$\tau_2 \text{ (s)}$	[0.154 ; 0.166]	[0.151 ; 0.168]	[0.143 ; 0.168]
ε_∞	[2.999 ; 3.001]	[2.999 ; 3.001]	[2.999 ; 3.001]
C.T.	4h 8min	4h 35min	10h 14min

5. CONCLUSIONS

In this paper, we endeavoured to show that a bounded error identification technique, based on the use of interval analysis could be an interesting alternative to classical estimation techniques for the analysis of dielectric relaxation spectra. Indeed, these methods allow one to obtain guaranteed estimation of the model parameters and of their associated uncertainties. Furthermore, in some cases it makes it possible to invalidate the model used.

Finally, we hope that this method will allow one to obtain reliable values of Havriliak-Negami model parameters and thus to obtain accurate information on the distribution function of relaxation times, particularly when several dipole contributions are observed in the measurement frequency range. Nevertheless, some improvements must be made in order to reduce the computing time, thus rendering tractable the use of actual data.

REFERENCES

1. A.R. Blythe, *Electrical Properties of Polymers*, University Press, Cambridge, 1979.
2. R. Coelho and B. Aladenize, *Les Diélectriques*, Hermès, Paris, 1993.
3. S. Havriliak Jr. and S.J. Havriliak, *Dielectric and Mechanical Relaxation in Materials*, Hanser, Munich, 1997.
4. R. E. Moore, *Interval Analysis*, Prentice Hall, New Jersey, 1966.
5. L. Jaulin and E. Walter, Set inversion via interval analysis for non-linear bounded-error estimation. *Automatica* (1993) **29**, 1053-1064.
6. E. Davis, Constraint propagation with interval labels. *Artificial Intelligence* (1987) **32**, 281-331.
7. L. Jaulin, M. Kieffer, O. Didrit and E. Walter, *Applied Interval Analysis*, Springer, Berlin, 2001.
8. L. Jaulin, Interval constraint propagation with application to bounded-error estimation. *Automatica* (2000) **36**, 1547-1552.
9. A. Neumaier, *Interval Methods for Systems of Equations*, Cambridge University Press, Cambridge, 1990.